A new mouse model of ARX dup24 recapitulates the patients' behavioral and fine motor alterations

Aline Dubos, Hamid Meziane, Giovanni Iacono, Aurore Curie, Fabrice Riet, Christelle Martin, Nadège Loaec, Marie-Christine Birling, Mohammed Selloum, Elisabeth Normand, et al.

Human Molecular Genetics, 2018, Vol. 27, No. 12 2138–2153

doi: 10.1093/hmg/ddy122
Advance Access Publication Date: 5 April 2018
Original Article

ORIGINAL ARTICLE

A new mouse model of ARX dup24 recapitulates the patients' behavioral and fine motor alterations

Aline Dubos[1,2,3,4], Hamid Meziane[4], Giovanni Iacono[5], Aurore Curie[6], Fabrice Riet[4], Christelle Martin[7], Nadège Loaëc[8], Marie-Christine Birling[4], Mohammed Selloum[4], Elisabeth Normand[7,9], Guillaume Pavlovic[4], Tania Sorg[4], Henk G. Stunnenberg[5], Jamel Chelly[1,2,3,10], Yann Humeau[7], Gaëlle Friocourt[8,†,*] and Yann Hérault[1,2,3,4,†,*]

[1]Institut de Génétique et de Biologie Moléculaire et Cellulaire, Université de Strasbourg, 67404 Illkirch, France, [2]Centre National de la Recherche Scientifique, UMR7104, 67404 Illkirch, France, [3]Institut National de la Santé et de la Recherche Médicale, U1258, 67404 Illkirch, France, [4]CELPHEDIA, PHENOMIN, Institut Clinique de la Souris, 67404 Illkirch, France, [5]Department of Molecular Biology, Radboud Institute for Molecular Life Sciences, Radboud University, 6500 HB Nijmegen, The Netherlands, [6]Centre de Référence Déficiences Intellectuelles de Causes Rares, Hôpital Femmes Mères Enfants, Hospices Civils de Lyon, Institut des Sciences Cognitives, CNRS UMR5304, Université Claude Bernard Lyon1, 69675 Bron, France, [7]Team Synapse in Cognition, Institut Interdisciplinaire de NeuroScience, Centre National de la Recherche Scientifique CNRS UMR5297, Université de Bordeaux, 33077 Bordeaux, France, [8]Inserm UMR 1078, Université de Bretagne Occidentale, Faculté de Médecine et des Sciences de la Santé, Etablissement Français du Sang (EFS) Bretagne, CHRU Brest, Hôpital Morvan, Laboratoire de Génétique Moléculaire, 29200 Brest, France, [9]Pole In Vivo, Institut Interdisciplinaire de NeuroScience, Centre National de la Recherche Scientifique CNRS UMR5297, Université de Bordeaux, 33077 Bordeaux, France and [10]Service de Diagnostic Génétique, Hôpital Civil de Strasbourg, Hôpitaux Universitaires de Strasbourg, 67091 Strasbourg, France

*Correspondence to be addressed. Tel: +33 0298018387; Fax: +33 0298016474; Email: gaelle.friocourt@univ-brest.fr (G.F.); Tel: +33 0388655715; Fax: +33 0388655690; Email: herault@igbmc.fr (Y.H.)

Abstract

The aristaless-related homeobox (ARX) transcription factor is involved in the development of GABAergic and cholinergic neurons in the forebrain. *ARX* mutations have been associated with a wide spectrum of neurodevelopmental disorders in humans, among which the most frequent, a 24 bp duplication in the polyalanine tract 2 (*c.428_451dup24*), gives rise to intellectual disability, fine motor defects with or without epilepsy. To understand the functional consequences of this mutation, we generated a partially humanized mouse model carrying the *c.428_451dup24* duplication ($Arx^{dup24/0}$) that we characterized at the behavior, neurological and molecular level. $Arx^{dup24/0}$ males presented with hyperactivity, enhanced stereotypies and

[†]These authors contributed equally to this work.
Received: November 25, 2017. **Revised:** February 22, 2018. **Accepted:** March 26, 2018

altered contextual fear memory. In addition, $Arx^{dup24/0}$ males had fine motor defects with alteration of reaching and grasping abilities. Transcriptome analysis of $Arx^{dup24/0}$ forebrains at E15.5 showed a down-regulation of genes specific to interneurons and an up-regulation of genes normally not expressed in this cell type, suggesting abnormal interneuron development. Accordingly, interneuron migration was altered in the cortex and striatum between E15.5 and P0 with consequences in adults, illustrated by the defect in the inhibitory/excitatory balance in $Arx^{dup24/0}$ basolateral amygdala. Altogether, we showed that the *c.428_451dup24* mutation disrupts *Arx* function with a direct consequence on interneuron development, leading to hyperactivity and defects in precise motor movement control and associative memory. Interestingly, we highlighted striking similarities between the mouse phenotype and a cohort of 33 male patients with *ARX c.428_451dup24*, suggesting that this new mutant mouse line is a good model for understanding the pathophysiology and evaluation of treatment.

Introduction

So far, more than 100 mutations have been identified in human in the aristaless-related homeobox (ARX) transcription factor encoding gene, located on the X chromosome. Depending on the phenotypic severity, *ARX* mutations can be divided into two groups: (i) a group with brain malformations, including X-linked lissencephaly with abnormal genitalia (1–3), hydranencephaly with abnormal genitalia and Proud syndrome (4), and (ii) a group without brain malformation, comprising X-linked intellectual disability (ID) with or without epilepsy and Partington syndrome (ID and dystonic movements of the hands) (see for reviews 5–7).

ARX is involved in GABAergic neuron development in the cortex, hippocampus and basal ganglia, and in cholinergic neuron development in the striatum, medial septum and ventral forebrain nuclei (2,5,8,9). Accordingly, its expression is controlled by *Dlx* transcription factors (10,11), which are important for the differentiation of telencephalic GABAergic neurons (12) and it regulates the expression of several genes important for brain development, in particular interneuron development (13–16).

ARX protein contains a homeodomain implicated in DNA binding, an aristaless domain at the C-terminus, responsible for transcriptional activation, an octapeptide domain close to the N-terminus, involved in transcriptional repression, and four polyalanine tracts whose function is not well known (17). Interestingly, the majority of *ARX* mutations affects the two first polyalanine tracts of ARX protein. In particular, the in-frame 24 bp duplication (*c.428_451dup24*), that expands the normal 12 polyalanine tract 2 to 20 (aa 144–155), occurs in 67–76% of unrelated *ARX* mutated patients without brain malformation (7,18). Originally, the *c.428_451dup24* mutation was reported to cause variable phenotypes, including West syndrome, Partington syndrome and non-syndromic X-linked ID. However, recent clinical re-evaluation of *c.428_451dup24* patients suggested that this mutation constitutes a recognizable clinical syndrome with ID, an oro-lingual apraxia and a very specific upper limb distal motor apraxia associated with a pathognomonic handgrip and variable epilepsy expression (19).

So far, the effect of *ARX* polyalanine expansions is not well understood. Overexpression experiments have suggested that they may cause protein aggregation and subsequent increased cell death in transfected cells (5,20,21) although two studies in transgenic mice for two different expansions in *ARX* polyalanine tracts [*c.304ins(GCG)*$_7$ and *c.428_451dup24*] have reported the absence of detectable protein aggregates or cell death *in vivo* (22,23). More recently, ARX polyalanine expansions have been shown to spontaneously promote the inappropriate self-assembly of these sequences into α-helical clusters with diverse oligomeric states, likely leading to the disruption of normal protein interactions (24). It has also been suggested that polyalanine expansions may affect directly ARX transcription activity. ARX can act both as a transcriptional repressor and activator (17,25). *In vitro* studies suggested that polyalanine expansions result in an increased repression activity (17). In contrast, studies in transfected cells showed less or decreased repression of some ARX known target genes with *c.304ins(GCG)*$_7$ and *c.428_451dup24*, suggesting a partial loss-of-function effect (6,26,27). Nevertheless, it is more likely that these polyalanine expansions result in the misregulation of a subset of target genes, as shown for *c.304ins(GCG)*$_7$ mutation in mice (26).

To better understand the *in vivo* effect of polyalanine expansions on ARX functions, two mouse models for the *c.304ins(GCG)*$_7$ mutation have been generated (22,23) and their phenotypes were very similar to human patients. So far, only one model has been generated for the *c.428_451dup24* (called dup24) mutation and was reported to have no major phenotype (23), although some of ARX target genes were found misregulated in these mice (27). Unlike the previous dup24 mouse model which was created by the insertion of 24 bp expansion in the polyalanine tract 2 of the mouse *Arx* gene (23), we here generated and characterized a new partially humanized knock-in mouse line carrying part of human *ARX* exon 2 coding for the polyalanine tract 1 and the expanded polyalanine tract 2.

Results

Decreased *Arx* mRNA and protein expression in $Arx^{dup24/0}$ mutant brains

The $Arx^{dup24/0}$ mutant mouse line was generated as described in Figure 1A and B and the Supplementary Material. Interestingly, we found that the polyalanine tract 2 containing the duplication of 24 bp is rather unstable at the DNA level and can result in mosaicism in a small fraction of cells (see Supplementary Material, Fig. S1).

Brains from $Arx^{dup24/0}$ males looked normal in size and did not show any gross malformation at E15.5, P0 and in adult (Supplementary Material, Fig. S2A–F). However, when we looked at ARX expression at E15.5 by immunohistochemistry, we noticed that ARX+ cells were generally less strongly labeled in the brain of $Arx^{dup24/0}$ than $Arx^{wt/0}$ mice (Supplementary Material, Fig. S2G and H), suggesting a reduction of the amount of ARX protein. To confirm this observation, we quantified *Arx* mRNA and protein in $Arx^{dup24/0}$ and $Arx^{wt/0}$ E15.5 forebrains. We observed a slight but significant reduction of *Arx* mRNA in $Arx^{dup24/0}$ mice (Fig. 1C) and a 23% reduction of ARX protein in $Arx^{dup24/0}$ mice (Fig. 1D and E), which is consistent with 8–50% decreased protein amount reported in another mouse model for the same mutation (27). We also quantified *Arx* expression in adult brain, and found a similar decrease at the mRNA level which however did not reach statistical significance (ratio *Arx*

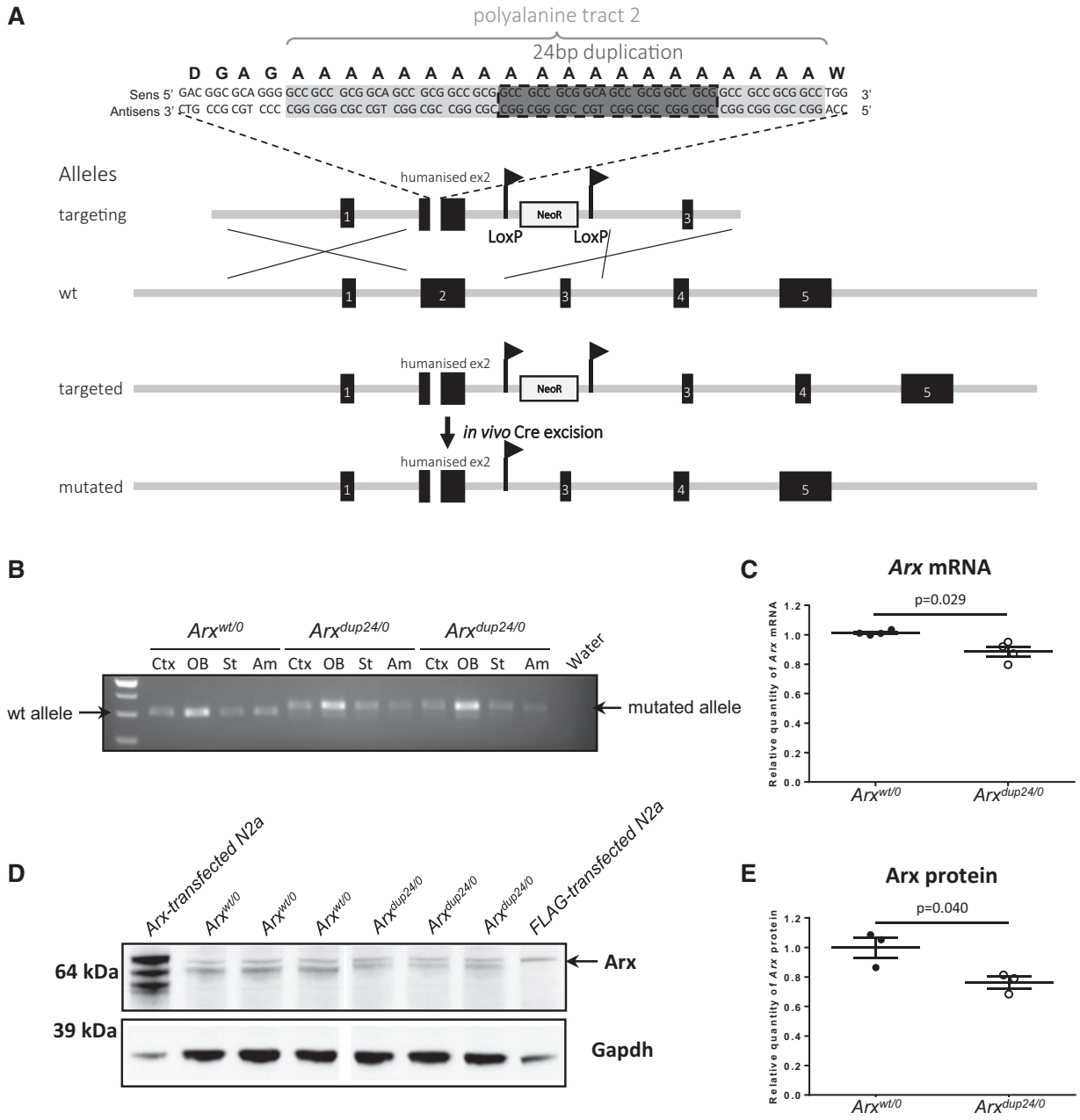

Figure 1. Generation of *Arx* knock-in mouse line ($Arx^{dup24/0}$). (**A**) A targeting vector containing a partially humanized mouse exon 2 fragment (corresponding to human *ARX* amino-acid 79–160) carrying the human *c.428_451dup24* mutation was generated and electroporated into male 129sv pass ES cells to obtain the targeted allele. The floxed Neo selection cassette was removed *in vivo* by direct breeding of the chimaeras with a CMV-Cre deleter line. The Cre transgene was segregated by a further breeding step. (**B**) Detection of wild-type (wt) and mutated alleles by RT-PCR in four different adult brain regions (cortex, olfactory bulb, striatum and amygdala) from one $Arx^{wt/0}$ and two $Arx^{dup24/0}$ males, respectively. Note that we observed a band below the band corresponding to the mutated allele which was probably the result of the instability of the polyalanine tract 2 with the 24 bp duplication (see Supplementary Material). (**C**) Graph showing the expression levels of *Arx* mRNA in four $Arx^{wt/0}$ and four $Arx^{dup24/0}$ E15.5 males normalized to the mean expression level in $Arx^{wt/0}$ males. A significant reduction of *Arx* mRNA expression was observed by qRT-PCR in $Arx^{dup24/0}$ E15.5 forebrain ($Arx^{wt/0}$: 1.01±0.01, n=4 versus $Arx^{dup24/0}$: 0.88±0.06, n=4, P=0.029, unpaired t-test). (**D**) Western blot showing Arx expression in three $Arx^{dup24/0}$ and three $Arx^{wt/0}$ E15.5 mouse forebrains. Semi-quantification was performed on Arx specific band, corresponding to the lower band (shown by the arrow) and which is absent in the negative control. N2a cells transfected with *Arx* cDNA or FLAG cDNA were used as positive and negative controls, respectively. Note that we detected a shift in the size of Arx protein (due to the presence of the 24 bp duplication) in the three $Arx^{dup24/0}$ mice when compared to the three $Arx^{wt/0}$ mice. (**E**) Graph showing the quantification of Arx protein expression in western blot normalized to Arx protein expression in $Arx^{wt/0}$ males. A significant reduction of Arx protein expression in $Arx^{dup24/0}$ E15.5 forebrain was observed by protein dosage on the western blot ($Arx^{wt/0}$: 1.00±0.12, n=3 versus $Arx^{dup24/0}$: 0.76± 0.07, n=3, P=0.040, unpaired t-test). Ctx: cortex, OB: olfactory bulb, St: striatum, Am: amygdala.

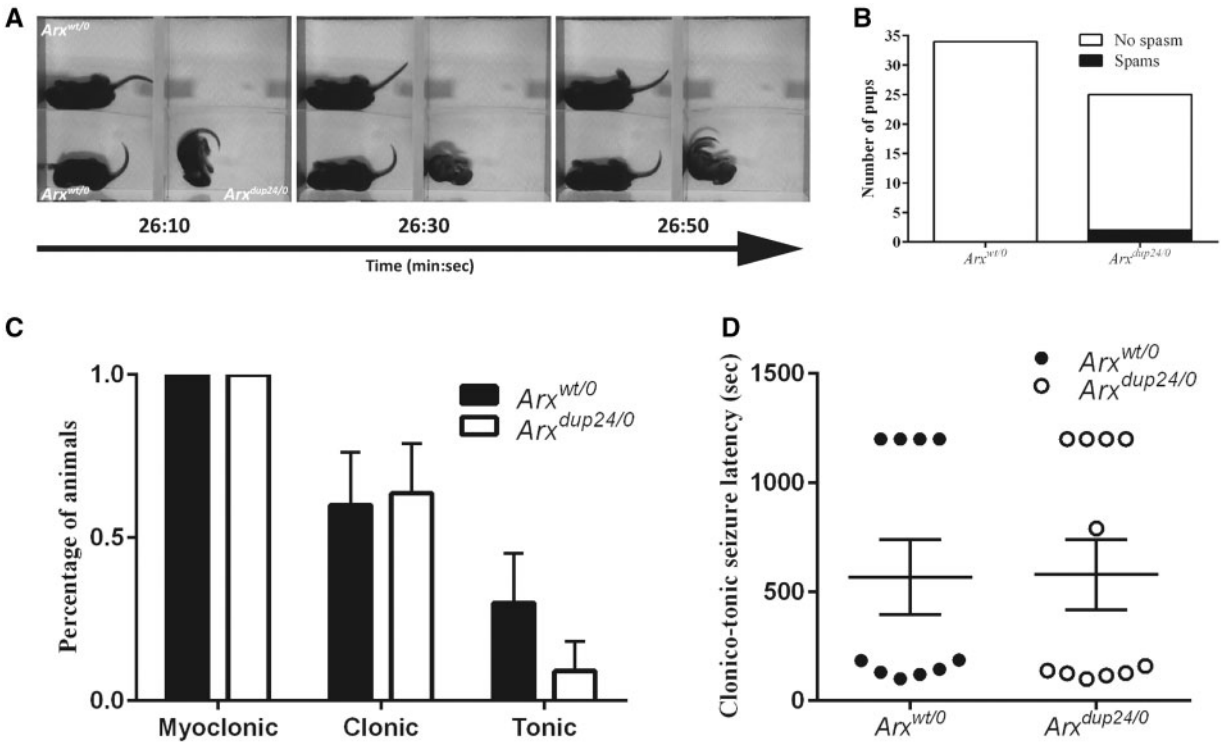

Figure 2. Eight percent of $Arx^{dup24/0}$ pups present with infantile spasms, however adult $Arx^{dup24/0}$ mice have comparable seizure susceptibility than $Arx^{wt/0}$ mice after PTZ injection. (**A**) Still frames selected from a digital video recording of two $Arx^{wt/0}$ and one $Arx^{dup24/0}$ pups depicting an $Arx^{dup24/0}$ pup of 9 days old (bottom row) having motor spasms during more than 20 sec involving sustained flexion of all limbs (left panel). (**B**) Major spasms were observed in 2 out of 25 $Arx^{dup24/0}$ pups, but were never observed in any of the 34 $Arx^{wt/0}$ pups. (**C** and **D**) Quantification of the seizures susceptibility in $Arx^{wt/0}$ and $Arx^{dup24/0}$ mice after injection of 50 mg/kg of pentylenetetrazol (PTZ). (**C**) The percentage of animals showing myoclonic, clonic or tonic seizures was similar between $Arx^{dup24/0}$ and $Arx^{wt/0}$ mice. (**D**) The latency of seizure appearance was also comparable between the two genotypes.

mRNA in $Arx^{dup24/0}$ versus $Arx^{wt/0}$: 0.88 ± 0.15, $n = 4$, $P = 0.47$, unpaired *t*-test). Unfortunately, the level of ARX protein was too low in adult to allow a precise quantification by western blot.

Eight percent of $Arx^{dup24/0}$ pups presented with infantile spams, but no increased susceptibility to induced epilepsy in adult

As infantile spasms were occasionally described in *ARX c.428_451dup24* patients (28), we tested $Arx^{dup24/0}$ males for the presence of infantile spontaneous motor spasms at P7, P9 and P11 during 30 min by video-monitoring. None of the 34 $Arx^{wt/0}$ pups displayed any spontaneous motor spasms, whereas two of the 25 $Arx^{dup24/0}$ pups (corresponding to 8% of $Arx^{dup24/0}$ pups) showed spasms (Fig. 2A and B). In addition, we tested the susceptibility of adult $Arx^{dup24/0}$ males to seizures induced by injection of a pro-convulsive agent, the pentylenetetrazole (PTZ). When a dose of 50 mg/kg of PTZ was administered intraperitoneally to mice, no difference in susceptibility to seizures was observed between $Arx^{wt/0}$ and $Arx^{dup24/0}$ mice. Myoclonic, clonic and tonic seizures frequencies (clonic: $\chi^2 = 0.029$, $P = 0.864$; tonic: $\chi^2 = 1.485$, $P = 0.223$; death: $\chi^2 = 1.485$, $P = 0.223$, Chi square test), as well as the latency of clonico-tonic seizure (clonico-tonic latency: $t_{19} = 0.046$, $P = 0.964$, Student *t*-test) were comparable between genotypes (Fig. 2C and D), suggesting that adult $Arx^{dup24/0}$ males do not have increased susceptibility to seizures.

$Arx^{dup24/0}$ males show hyperactivity and alteration of contextual fear conditioning

ARX c.428_451dup24 patients present a variety of neurological and behavioral manifestations (19; this study), thus we investigated our mouse model for those manifestations. $Arx^{dup24/0}$ males had normal physical appearance and body weight and did not show any obvious sign of altered sensory or vestibular functions. The locomotor activity was increased in $Arx^{dup24/0}$ as compared to $Arx^{wt/0}$ males in several tests as shown by the higher: (i) distance travelled in the open field arena {[$F(1, 20) = 5.92$, $P = 0.025$, repeated measures ANOVA]; $P < 0.05$ for 10, 15 and 20 min time points with Student *t*-test} (Fig. 3A), (ii) number of visited arms in the Y maze ($t_{20} = 3.69$, $P = 0.0015$, Student *t*-test) (Fig. 3B) and (iii) total number of entries in the chambers in the social recognition test ($t_{20} = 1.75$, $P = 0.095$, Student *t*-test) (Supplementary Material, Fig. S3A). $Arx^{dup24/0}$ mutants also showed increased vertical activity (rearing) in the open field {[$F(1, 20) = 9.41$, $P = 0.006$, repeated measures ANOVA]; $P < 0.05$ for 10–30 min time points with Student *t*-test} (Fig. 3A) and throughout the testing period of the circadian activity ($t_{20} = 1.99$, $P = 0.061$, Student *t*-test) (Fig. 3C). Altogether, we found that $Arx^{dup24/0}$ males displayed hyperactivity and enhanced stereotypy (illustrated by rearing activity), particularly in new environments.

We then performed different assays to assess social and emotional behavior and learning and memory abilities of $Arx^{dup24/0}$ mutants (see Supplementary Material, Fig. S3). In the

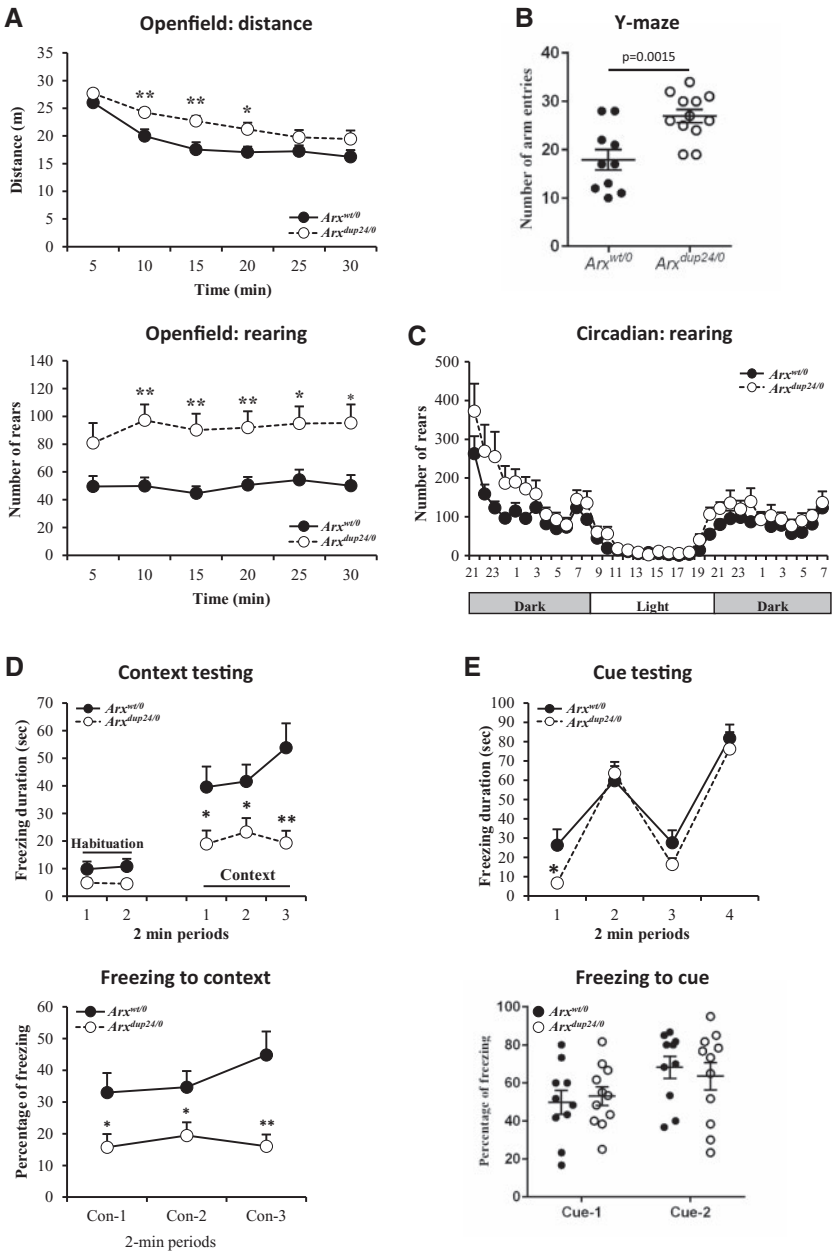

Figure 3. $Arx^{dup24/0}$ males presented with hyperactivity and alteration of contextual fear conditioning. (**A–D**) Hyperactivity was observed in several tests. (A) In the open-field, the distance travelled (t_{20} =2.43, $P<0.05$) (upper panel) and the number of rears (lower panel) were significantly increased in $Arx^{dup24/0}$ compared to $Arx^{wt/0}$ mice. (B) In the Y-maze, the number of visited arms was significantly increased in mutants. (C) $Arx^{dup24/0}$ males showed increased vertical activity throughout the light/dark cycle when compared to $Arx^{wt/0}$ males. (D) In the fear conditioning paradigm, when animals were re-exposed in the same context 24 h after conditioning, both genotypes showed increased freezing compared to baseline, however contextual freezing performance was significantly decreased in $Arx^{dup24/0}$ mutants. Note that $Arx^{dup24/0}$ males tended to have lower baseline levels of immobility during habituation than $Arx^{wt/0}$ mice. (**E**) However, when animals were placed in a new context, $Arx^{dup24/0}$ mice showed same cued freezing performance than $Arx^{wt/0}$. Note that $Arx^{dup24/0}$ mice showed decreased baseline immobility compared to $Arx^{wt/0}$ males, but not when testing for cue memory. *$P<0.05$, **$P<0.01$ versus wt.

fear conditioning test, $Arx^{dup24/0}$ mutants exposed to the conditioning cage tended to have lower baseline levels of immobility than $Arx^{wt/0}$ mice during the habituation [$F(1, 19) = 3.72$, $P = 0.069$, repeated measures ANOVA] (Fig. 3D), which could be attributed to their hyperactivity. When animals were re-exposed to the same context 24 h after conditioning, both $Arx^{wt/0}$ and $Arx^{dup24/0}$ mice showed significantly, but differently, increased freezing as compared to the baseline [pre–post conditioning: $F(1, 19) = 31.97$, $P < 0.0001$; interaction genotype*time $F(1, 19) = 3.58$, $P = 0.074$; genotype: $F(1, 19) = 6.44$, $P = 0.020$; repeated ANOVA on the last 2 min of habituation and the first 2 min of context] (Fig. 3D). Indeed, contextual freezing performance was significantly lower in $Arx^{dup24/0}$ mutants as compared to $Arx^{wt/0}$ counterparts {[$F(1, 19) = 10.10$, $P = 0.005$, repeated measures ANOVA]; $P < 0.05$ for each time point, Student *t*-test}. When animals were placed in a new context, $Arx^{dup24/0}$ mutants still had lower baseline immobility than $Arx^{wt/0}$ ($t_{19} = 2.43$, $P = 0.025$, Student *t*-test) (Fig. 3E). Presentation of conditional stimuli alone in the new context induced in both genotypes a clear fear reaction, reflected by a comparable cued freezing

performance between genotypes [F(1, 19) = 0.009, $P = 0.926$, repeated measures ANOVA] (Fig. 3E) and excluding the possibility that $Arx^{dup24/0}$ males' hyperactivity was responsible for the alteration in the contextual memory. Altogether, these data suggest specific alteration of contextual memory for fear in $Arx^{dup24/0}$ mice.

$Arx^{dup24/0}$ males show altered fine motor and proprioceptive abilities

In order to determine if our mouse model recapitulates the fine motor phenotypes observed in *ARX c.428_451dup24* patients (19; this study), we evaluated the fine motor skills. Beforehand, we assessed mouse muscle strength with the grip test and their traction force in the string test and did not observe any differences between $Arx^{dup24/0}$ and $Arx^{wt/0}$ mice (grip strength: $t_{19} = 1.08$, $P = 0.294$; traction force: $t_{19} = -1.06$, $P > 0.05$, Student *t*-test), suggesting normal muscle strength in mutant mice (Supplementary Material, Fig. S3B). We then performed the mouse reaching and grasping (MoRaG) test (29,30). Both $Arx^{wt/0}$ and $Arx^{dup24/0}$ were highly lateralized, using either the left or the right paw to proceed [lateralization: F(2, 94) = 15.48, $P < 0.0001$; interaction genotype*lateralization F(2, 94) = 2.73, $P = 0.071$; repeated measures ANOVA on the three sessions] (Fig. 4A). Interestingly, over the three testing sessions, $Arx^{dup24/0}$ mice showed significantly decreased accuracy of reaching {[F(1, 47) = 7.54, $P = 0.009$, repeated ANOVA]; $P < 0.01$ for day 2 and 3 Student *t*-test} and grasping {[F(1, 47) = 13.07, $P = 0.0007$, repeated ANOVA, followed by Student *t*-test for each day $P < 0.05$]; $P < 0.05$ for each day Student *t*-test} than $Arx^{wt/0}$ mice (Fig. 4A), suggesting that $Arx^{dup24/0}$ mice have altered precision in movement toward the target and deficient fine-tuned grasping ability. In addition, we evaluated gait of $Arx^{dup24/0}$ versus $Arx^{wt/0}$ mice. In the beam walking test, $Arx^{dup24/0}$ mice took as much time as $Arx^{wt/0}$ mice to cross the beam distance ($t_{17} = 1.18$, $P = 0.254$, Student *t*-test), but showed significantly higher number of slips than $Arx^{wt/0}$ mice ($t_{17} = 2.94$, $P = 0.009$, Student *t*-test) (Fig. 4B). Automated gait analysis revealed that $Arx^{dup24/0}$ mice have several fine lateralized motor changes with increased: (i) right hind paw stance duration ($t_{14} = 2.14$, $P = 0.050$, Student *t*-test) (Fig. 4C), (ii) left forelimb brake duration ($t_{14} = 2.32$, $P = 0.036$, Student *t*-test) (Fig. 4C) and (iii) left hind paw propel duration ($t_{14} = 2.18$, $P = 0.047$, Student *t*-test) (Fig. 4C); as if the higher propulsion was compensated by higher brake in mutants. $Arx^{dup24/0}$ mice also had increased step angle for the forepaws ($t_{14} = 3.11$, $P = 0.008$, Student *t*-test) (Fig. 4C). The gait parameters were even more affected in a second older cohort (15–31 weeks old) where all limbs had increased stance and propel duration ($t_{17} \geq 2.12$, $P < 0.05$, Student *t*-test; Supplementary Material, Fig. S3H). Finally, we analyzed $Arx^{dup24/0}$ mice for specific motor coordination. $Arx^{dup24/0}$ mice showed significantly higher latencies to fall from the rotarod than $Arx^{wt/0}$ mice ($t_{19} = 2.19$, $P = 0.042$; Student *t*-test) (Supplementary Material, Fig. S3C), suggesting improved motor coordination of $Arx^{dup24/0}$ mice. It is possible that as $Arx^{dup24/0}$ mutants are more active than $Arx^{wt/0}$, they manage to better anticipate the increase in the rotation speed, which leads to a better performance at the rotarod than $Arx^{wt/0}$ mice. Altogether, these results suggest that $Arx^{dup24/0}$ mice present alteration of fine motor and proprioceptive abilities without major impact on coordination.

Down-regulation of interneuron specific genes in $Arx^{dup24/0}$ forebrain at E15.5

To gain better insights into the molecular consequences associated with the 24 bp duplication, we performed genome-wide RNA sequencing (RNA-seq) on embryonic E15.5 forebrains from $Arx^{dup24/0}$ and $Arx^{wt/0}$ males and found 255 and 171 genes significantly up- and down-regulated in $Arx^{dup24/0}$ mice, respectively (*DEseq2* algorithm, exon reads, $P < 0.025$ and Supplementary Material, Table S2). Pathway analysis unraveled major differences between up- and down-regulated genes (Fig. 5A): while down-regulated genes were endowed with synaptic transmission-related functions, up-regulated genes were mostly related to various aspects of central nervous system development and DNA interaction (Fig. 5A). Of note, some of the previously identified *Arx* target genes (*Lmo1*, *Lmo3*, *Lmo4*, *Shox2*, *Gbx2*, *Lhx7/8*, *Ebf3*, *Rasgef1b*; (13–15)) were not found significantly deregulated in $Arx^{dup24/0}$ E15.5 forebrains.

To relate our results to GABAergic interneuron (IN) development for which *Arx* is known to be important, we took advantage of three previous experimental datasets (31–33), which investigated genes specifically expressed (markers) or silenced in GABAergic INs. We found down-regulated genes highly enriched in interneuron markers, namely cortical (E13 $P < 1.4e{-}21$, E14 $P < 7.8e{-}19$, hypergeometric test, Bonferroni correction) and ganglionic eminence (GE) IN precursors (E14 $P < 4.6e{-}36$, hypergeometric test, Bonferroni correction) or mature IN (P30 $P < 4.2e{-}9$, hypergeometric test, Bonferroni correction) (Fig. 5B). In contrast, up-regulated genes were enriched in genes normally silenced in IN (E13 $P < 8e{-}87$, E14 $P < 2.1e{-}76$, hypergeometric test, Bonferroni correction; Fig. 5B) with enrichment scores consistent amongst the three datasets. Moreover, we found a strong correlation between the specificity of IN markers and the degree of enrichment in $Arx^{dup24/0}$ down-regulated genes and reciprocally between the specificity of IN silenced genes and the degree of enrichment in $Arx^{dup24/0}$ up-regulated genes (Fig. 5C). This suggests that the 24 bp duplication causes a specific down-regulation of highly specific IN markers and an up-regulation of genes not meant to be expressed in INs in normal conditions. To ensure the reliability of our RNA-seq results, a subset of dysregulated genes were selected and analyzed in E15.5 forebrains of $Arx^{dup24/0}$ and $Arx^{wt/0}$ control littermates using real-time quantitative polymerase chain reaction (RT-qPCR). For all genes analyzed, RT-qPCR results confirmed the deregulation observed in RNA-seq experiments, although not always with the same magnitude or level of statistical significance (Fig. 5D).

Delayed interneuron development in $Arx^{dup24/0}$ forebrains

As our RNA-seq results suggested a perturbation of IN development, we thus investigated GABAergic IN populations at E15.5 using different IN markers to examine the number of labeled positive cells per mm^2 in different brain regions. The pattern of Calbindin (CB) labeling, a general marker of GABAergic INs, was similar in both localization and structures between $Arx^{dup24/0}$ and $Arx^{wt/0}$ males (Fig. 6A and B), however, there was a general decreased intensity of CB immunolabeling in $Arx^{dup24/0}$ E15.5 embryos, especially in the thalamus, hypothalamus and amygdala, consistent with the decreased *Calb1* expression observed in RNA-seq experiments at this stage. Although the number of CB+ cells per mm^2 was not changed in the mutant hippocampus, we found a decreased number of CB+ cells in the cortex,

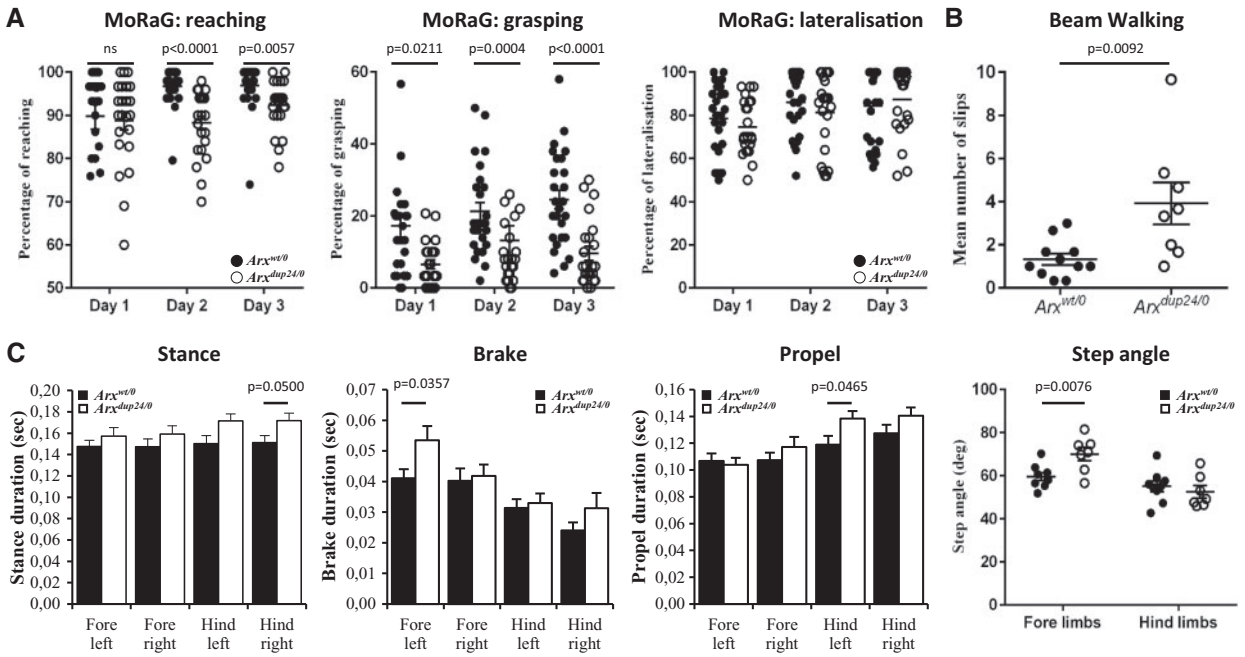

Figure 4. $Arx^{dup24/0}$ males presented impaired fine motor and proprioceptive abilities. (**A**) The mouse reaching and grasping (MoRaG) test allows to determine mouse front paw reaching and grasping abilities as well as which front paw (right or left) they use to perform the test. $Arx^{dup24/0}$ males had a decreased percentage of accurate reaching (left panel) and grasping (middle panel) than $Arx^{wt/0}$ mice. The percentage of lateralized mice was similar between $Arx^{dup24/0}$ and $Arx^{wt/0}$ mice (right panel). (**B**) Although they took the same time to cross the beam, $Arx^{dup24/0}$ males displayed increased number of slips in the beam walking test when compared to $Arx^{wt/0}$ males. (**C**) Automated gait analysis showed increased duration of the stance for the right hind paw (left panel) due to increased duration of the brake for the left fore-paw (middle left panel), and of the propel for the left hind paw (middle right panel). $Arx^{dup24/0}$ males also had an increased step angel for the forelimbs (right panel). *P <0.05, **P<0.01, ***P<0.001 versus wt.

the striatum and the amygdala of $Arx^{dup24/0}$ mice (Fig. 6C, D and G). Similar results were obtained with Calretinin (CR) immunolabeling (Fig. 6G). Next, we looked at CB+ and CR+ distribution in the different IN migration streams within the cortex. In the cortex of $Arx^{dup24/0}$ mice, we found no difference in the number of CB+ or CR+ cells in the marginal zone (MZ), but we observed a significant decrease in the number of CB+ or CR+ cells in the cortical plate (CP)/subplate (SP), as well as in the subventricular zone/intermediate zone (SVZ/IZ) of $Arx^{dup24/0}$ embryos compared to $Arx^{wt/0}$ embryos (Fig. 6E and F). Similar results were also observed with ARX+ cells (Supplementary Material, Fig. S2G and H). In contrast, we did not notice any change with somatostatin (SST) immunolabeling, which is consistent with the absence of deregulation of *Sst* in the RNA-seq experiments at this stage. Finally, there was a slight decreased number of Choline acetyltransferase (ChAT) expressing cells in $Arx^{dup24/0}$ mice that seemed to be restricted to the developing striatum and not to the other basal cholinergic nuclei (data not shown). We excluded that the decreased number of interneurons in the different brain regions was due to interneuron progenitor proliferation defect or increased cell apoptosis of interneurons as the number of phosphohistone 3 positive (PH3) cells in the ventricular zone of the GE and the number of cleaved caspase 3 positive cells within the brain were similar between $Arx^{dup24/0}$ and $Arx^{wt/0}$ embryos (PH3: $Arx^{wt/0}$: 535.2 ± 26.4 cells/mm^2 $n = 4$ versus $Arx^{dup24/0}$: 555.1 ± 31.1 cells/mm^2 $n = 5$, $P = 0.6518$, Student *t*-test). Taken together these results suggest that the 24 bp duplication in *Arx* gene induces a defect of IN migration in $Arx^{dup24/0}$ mice at E15.5, (i) from the GE to the cortex and to a lesser extent, to the hippocampus and (ii) from the GE to the subpallial structures including the striatum.

We then investigated glutamatergic neuronal populations at E15.5 using different projecting neuron markers including markers of radial glia cells (Pax6), intermediate progenitors (Tbr2) and post-mitotic neurons (Tbr1) in the cortex. We did not observe any difference in the number of Pax6+ and Tbr2+ cells, but we observed a small decrease (7.2%) in the number of Tbr1+ cells between $Arx^{wt/0}$ and $Arx^{dup24/0}$ E15.5 cortexes (Supplementary Material, Fig. S2I). In addition, as *Arx* loss-of-function in cortical progenitors has been shown to lead to proliferation defects (2,34,35), we labeled dividing progenitors in cortical ventricular and subventricular zones with an anti-PH3 antibody. However, the same number of PH3+ cells was observed both in the VZ and SVZ of $Arx^{wt/0}$ and $Arx^{dup24/0}$ E15.5 cortexes (Supplementary Material, Fig. S2I). Thus the 2 4bp duplication in *Arx* gene slightly reduced projecting neuron number but did not affect proliferation at this stage. We thus decided to focus on interneuron populations.

At P0 and adult stages, brain structures labeled with ARX, CB, CR, parvalbumin (PV) or SST appeared similar between $Arx^{dup24/0}$ and $Arx^{wt/0}$ mice. Furthermore, the total number of IN expressing these different markers was comparable between $Arx^{dup24/0}$ and $Arx^{wt/0}$ in the cortex, striatum and hippocampus (data not shown). However, at P0, we noticed changes in the distribution of ARX+, CB+, CR+ and SST+ cells in both somatosensoriel and motor cortexes, analyzed by dividing these cortical regions into 10 bins of the same size and counting the number of cells in each bin (Supplementary Material, Fig. S4A–H). We found less cells in central parts of the CP (bin 4, corresponding approximately to layer IV) and more cells in either the deeper part of the cortex (bin 7–10) and/or in upper parts of the cortex (bin 2–3) of $Arx^{dup24/0}$ (Fig. 6H), suggesting that migrating INs accumulate in the upper and deeper parts of the CP, as a possible result of defect in radial migration

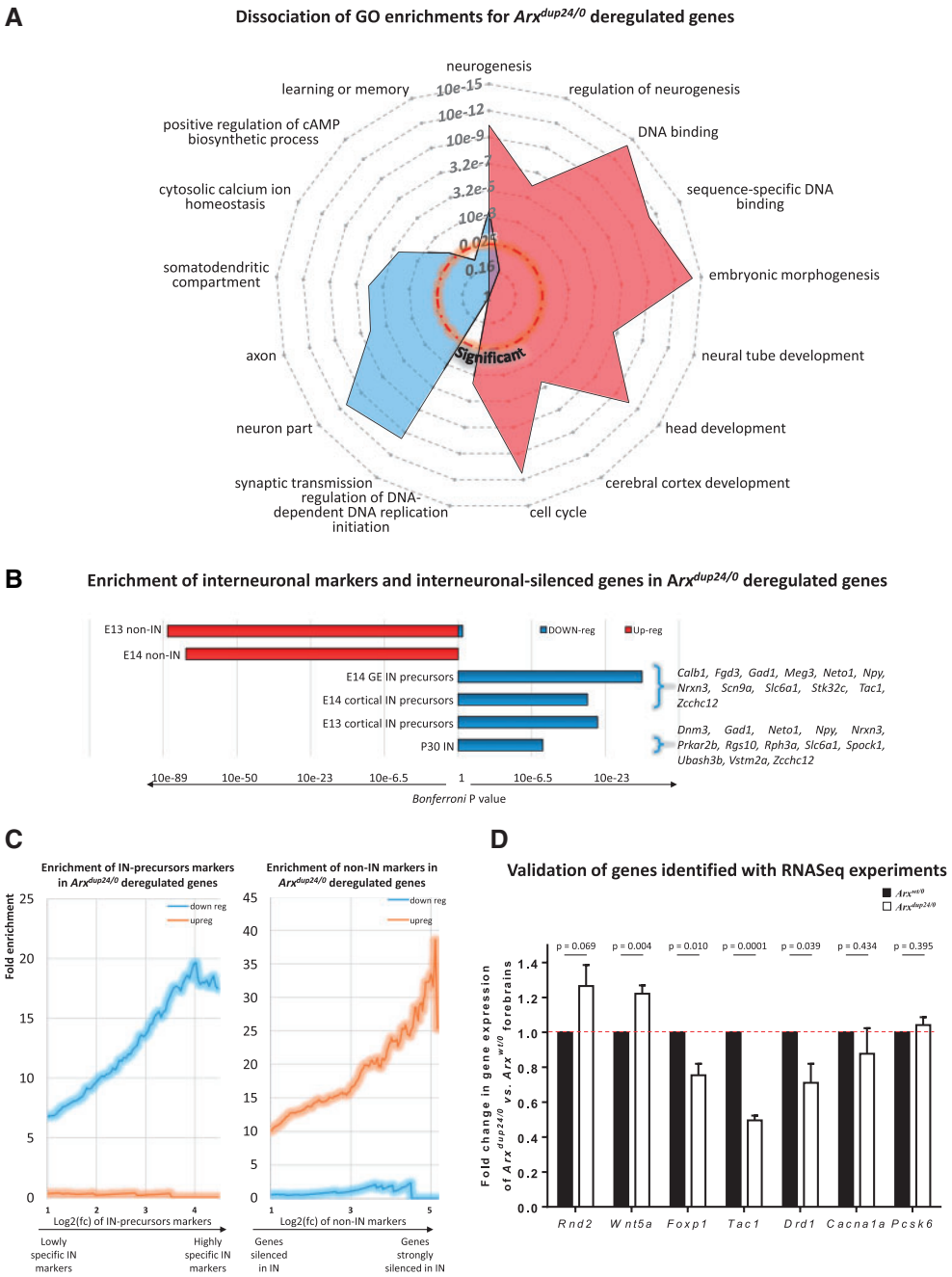

Figure 5. RNA-seq analysis of genes deregulated in $Arx^{dup24/0}$ E15.5 forebrain revealed interneuron development defects. (**A**) Gene ontology (GO) enrichments for deregulated genes. Radar plot in which outer rings correspond to more significant enrichments (Bonferroni corrected *P* values, *Z*-score scale). (**B**) Study of interneuronal (IN) markers and IN-silenced genes. Histogram of the Bonferroni corrected *P* values (hypergeometric enrichment) at E13 (32), E14 (31) and P30 (33). Some illustrative genes are shown on the right. (**C**) The 24 bp duplication impacts the hallmarks of neuronal identity. In each graph, Marsh's dataset was used to calculate IN-markers or IN-silenced genes with increasing specificity and $Arx^{dup24/0}$ deregulated genes were tested for enrichment against the progressive values of IN specificity. The left graph shows that the more we selected extremely specific IN markers (genes that are expressed only in IN and completely silenced in all other cell types) the more they were enriched in $Arx^{dup24/0}$ down-regulated genes. In other terms, $Arx^{dup24/0}$ may cause the down-regulation of the specific hallmarks that distinguish IN from other cell types, such as *Gad1* or *Npy*. The right graph shows the up-regulation of genes that were strongly meant to be silenced in interneurons. (**D**) Validation by RT-qPCR of seven genes identified by RNA-seq experiments in $Arx^{dup24/0}$ and $Arx^{wt/0}$ E15.5 forebrains. We observed similar changes in the expression level of tested genes, i.e. increased expression of *Rnd2* and *Wnt5a* genes and decreased expression of *Foxp1*, *Tac1*, *Drd1* and *Cacna1a* genes although not reaching statistical significance for *Rnd2* and *Cacna1a* (n=4 for each genotype, Student *t*-test). As observed in RNA-seq data, the expression of the *Pcsk6* gene was not changed in $Arx^{dup24/0}$ compared to $Arx^{wt/0}$ E15.5 forebrains.

into the CP following the tangential migration. In adult, these defects in cortical IN distribution were still present, but more subtle with ARX and CB markers and absent with CR, PV and SST markers (Fig. 6I). In the striatum of P0 mice, although there was no statistical difference between the number of ARX+, CB+ or CR+ cells, we observed a 22.8% decreased number of ChAT+ cells (Fig. 6J and Supplementary Material, Fig. S4I and J), which appeared to be specific of the striatum. The defect was still present

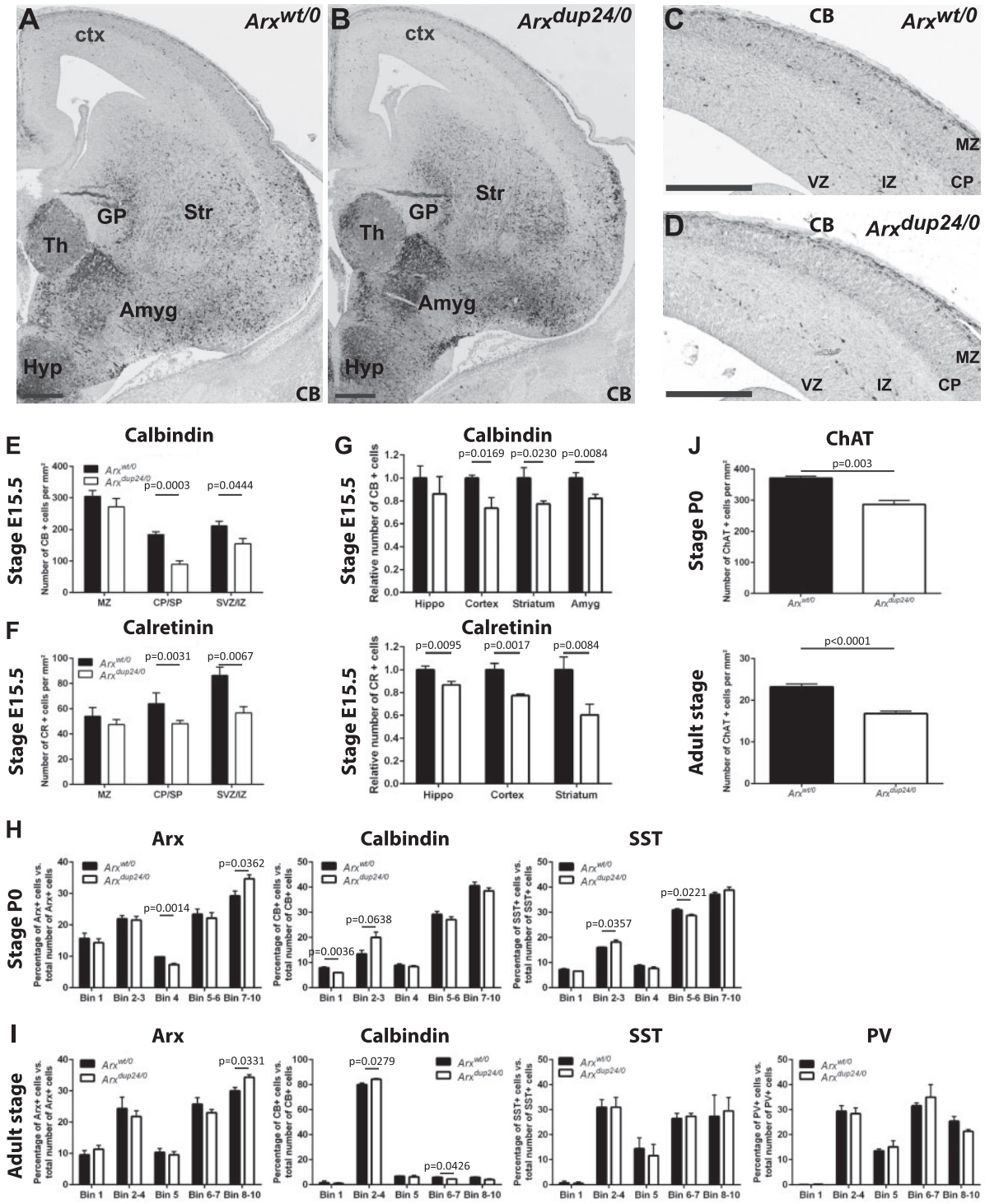

Figure 6. Expression and distribution of GABAergic interneuron markers at E15.5, P0 and in adult. (**A** and **B**) At E15.5, brain structures labeled with CB were similar between $Arx^{wt/0}$ (A) and $Arx^{dup24/0}$ (B) males. However, there was a strong decrease in the number of CB+ cells in the neocortex (**C** and **D**). (**E** and **F**) At early stages of cortical development, two streams of migrating IN can be identified in the pallium: one located just above the ventricular/subventricular (VZ/SVZ) surface and another positioned at the level of the marginal zone (MZ). Between E15.5 and E16.5, a third subplate (SP) stream forms between the SVZ/intermediate zone (IZ) and MZ streams. We thus looked at the number of CB+ and CR+ neurons in the different streams. (E) We observed a significant decrease in the number of CB+ cells in the subplate (SP)/cortical plate (CP) and in the subventricular zone (SVZ)/intermediate zone (IZ) of the cortex of $Arx^{dup24/0}$ compared to $Arx^{wt/0}$ mice (n=4 for $Arx^{wt/0}$, n=6 for $Arx^{dup24/0}$, Student t-test). (F) Similarly, although CR labeling was comparable between $Arx^{wt/0}$ and $Arx^{dup24/0}$ males, there was a decreased number of CR+ cells in the SP/CP and in the SVZ/IZ of the cortex of $Arx^{dup24/0}$ compared to $Arx^{wt/0}$ mice (n=4 for $Arx^{wt/0}$, n=5 for $Arx^{dup24/0}$, Student t-test). (**G**) Graphs showing the relative number of CB+ and CR+ cells in the hippocampus, cortex, striatum and amygdala for $Arx^{dup24/0}$ versus $Arx^{wt/0}$ males at E15.5 (Student t-test). (**H** and **I**) To analyze IN distribution at P0 and in adult, cortexes were divided into 10 bins of the same size covering the total thickness of the cortex. (H) At P0, bin 1 corresponds approximately to cortical layer I/II, bins 2 and 3 to layers II–IV, bin 4 to Layer IV, bins 5 and 6 to layer V and bins 7–10 to layer VI and white matter. Although there was no major difference between the number of positive cells in the cortex of $Arx^{dup24/0}$ compared to $Arx^{wt/0}$ animals, the distribution of Arx+ (H left panel), CB+ (H middle panel) and SST+ (H right panel)

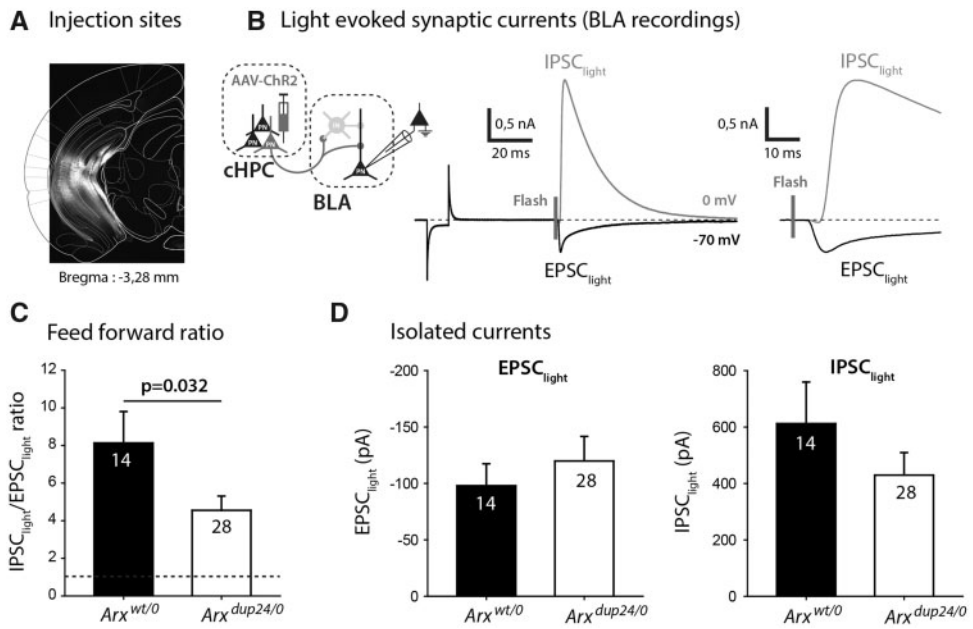

Figure 7. Electrophysiological recordings of hippocampal to basolateral amygdala connections revealed I/E imbalance in $Arx^{dup24/0}$ mice. (**A**) Intra hippocampal injections of ChR2-coding AAVs can be visualized by YFP-expression. (**B**) Application of short (1 ms duration) flashes of blue light on amygdala-containing acute slices to test for synaptic transmission at hippocampo-BLA projections. Light-evoked synaptic currents are recorded using whole cell patch clamp recordings of BLA neurons at appropriate membrane potentials. Light-evoked synaptic currents are shown at two time scales (left panel: 20 ms and right panel: 10 ms). Right panel: Note that a delay exists between excitatory (black line, −70 mV) and inhibitory currents (grey line, 0 mV), denoting the recruitment of local interneurons by incoming hippocampal fibers (feed-forward inhibition). (**C** and **D**) Amplitudes of light-evoked excitatory and inhibitory currents were measured in $Arx^{wt/0}$ (black bar) and $Arx^{dup24/0}$ (white bars) preparations. (C) I/E ratios are significantly decreased in $Arx^{dup24/0}$ neurons. (D) Separation of measured light-evoked currents allows to appreciate that the decrease in I/E ratios is mostly due to a decrease of light-evoked inhibitory currents (right panel). n=3 for $Arx^{wt/0}$, n=5 for $Arx^{dup24/0}$, Student t-test. Numbers of recorded cells are indicated.

in adult striatum where we noticed a 27.7% decreased of ChAT+ cells (Fig. 6J and Supplementary Material, Fig. S4K and L). Altogether, those results support RNA-seq data and show that the *c.428_451dup24* mutation leads to an alteration of GABAergic IN development during embryonic development. Although this alteration is partially rescued at P0 and in adult, we still observed subtle defects in cortical IN distribution and a specific reduction of ChAT+ cells in the striatum.

Inhibitory/excitatory imbalance at hippocampal to basolateral amygdala projections in adult $Arx^{dup24/0}$ males

Part of the developmental modifications observed in IN populations could explain the contextual fear conditioning alteration observed in adult $Arx^{dup24/0}$ animals. We previously demonstrated that hippocampal inputs to basolateral amygdala (BLA) neurons controlled the intensity of the conditioned fear response (36). To challenge this hypothesis, we tested the synaptic response of hippocampal projections to the BLA using optogenetic stimulation methods combined with electrophysiological detection of GABAergic synaptic currents in BLA neurons. Our aim was to examine if the *c.428_451dup24* mutation could redefine the inhibitory/excitatory (I/E) balance in this feed-forward neuronal circuit. To achieve this, we performed viral infection of the Channelrhodopsin-2 (ChR2) in caudal hippocampal neurons to allow expression of ChR2 in some BLA projecting neurons (Fig. 7A and B). We recorded light-evoked synaptic currents in BLA neurons at two membrane potentials allowing separating direct excitatory inputs from ChR2 expressing cells (at −70 mV) and indirect inhibitory inputs from recruited local INs which activation will give rise to GABAergic currents (at 0 mV) (Fig. 7B). The resulting I/E balance theoretically dictates the capacity of incoming long range inputs in activating downstream neurons.

Light-evoked excitatory potentials (EPSCs) were first compared by recording neurons at −70 mV, but their amplitude was not different between $Arx^{dup24/0}$ and $Arx^{wt/0}$ mice (Fig. 7D). We then recorded light-evoked inhibitory potentials at 0 mV, and observed a strong tendency toward a decrease in their amplitude in $Arx^{dup24/0}$ animals (Fig. 7D). However, the I/E balance at hippocampo-BLA afferents was significantly decreased by the 24 bp duplication (Fig. 7C). Thus, our results suggest that early development modifications in IN populations have functional consequences in adults, possibly contributing to the changes in contextual fear responses observed in $Arx^{dup24/0}$ adult mice.

cells was slightly different at P0 (n=4 for $Arx^{wt/0}$, n=4 for $Arx^{dup24/0}$, Student t-test). (I) In adult, bin 1 corresponds approximately to cortical layer I, bins 2–4 to layers II and III, bin 5 to Layer IV, bins 6 and 7 to layer V and bins 8–10 to layer VI and white matter. The distribution of Arx+ (I left panel) and CB+ (I middle panel) cells was slightly different in adult $Arx^{dup24/0}$ mice, but not for SST+ and PV+ cells (I right panel) (n=3 for $Arx^{wt/0}$, n=3 for $Arx^{dup24/0}$, Student t-test). (J) In the striatum, the number of ChAT+ neurons was decreased in $Arx^{dup24/0}$ compared to $Arx^{wt/0}$ mice at P0 (n=3 for $Arx^{wt/0}$, n=4 for $Arx^{dup24/0}$, Student t-test) (J left panel) and in adult (n=6 for $Arx^{wt/0}$, n=6 for $Arx^{dup24/0}$, Student t-test) (J right panel). Ctx: cortex, Str: striatum, GP: globus pallidus, Th: thalamus, Hyp: hypothalamus, Amyg: amygdala, VZ: ventricular zone, IZ: intermediate zone, CP: cortical plate, MZ: marginal zone, CB: calbindin. Scale bar: 250 μm.

Table 1. Comparison of phenotypes/clinical features observed in the partially humanized Arx dup24 mouse model and in human *ARX c.428_451dup24* patients

$Arx^{dup24/0}$ mice	*ARX c.428_451dup24* patients
Activity & behavior	
Hyperactivity in new environment (open field, Y-maze and social recognition test)	Hyperactivity in 47.6% of *ARX* patients (Nisonger's scale). Only 14.3% were assessed as being calm.
Normal anxiety level in the elevated plus maze and the open field	Only 19% of *ARX* patients have severe anxiety (>80th percentile, Nisonger's scale)
Increased rearing in the circadian activity & the open field, suggestive of stereotypy	Stereotypic behavior in 47.6% of *ARX* patients (Nisonger's scale)
Normal despair level in the tail suspension test	Depressive episode in only 11% of *ARX* patients (less frequent than in control population)
Normal social interaction	Despite their ID, 56.3% of *ARX* patients have perfectly adequate interpersonal relationship (Vineland adaptive behavioral scale)
Learning & memory	
	Mean IQ: 48, SD: 7, [40–70] (Wechsler scale)
Alteration of contextual fear memory	
Normal working memory in the Y-maze	Working memory index not significantly different from IQ (Wechsler scales).
Fine motor & proprioceptive abilities	
Defect in reaching in the MoRagTest	Impaired reaching component on a kinematic study of a grasping movement
Defect in grasping in the MoRagTest	Impaired grasping component on a kinematic study of a grasping movement
Increased performance on the rotarod, suggestive of improved motor coordination	Higher scores on the balance subtest of the LOMDS than IQ- and age-matched Down syndrome patients.
Normal muscle strength in the grip test	Normal muscle strength on motor examination.
Epilepsy	
Infantile spasms in 8% of $Arx^{dup24/0}$ pups	9.1% of *ARX* patients presented with West syndrome (mean age onset: 5 months, [4–7])

IQ, intelligence quotient.

$Arx^{dup24/0}$mice reflect phenotypes observed in c.428_451dup24 ARX patients

In order to determine to what extent the phenotype is similar between mouse model and human patients, we investigated 33 French patients carrying the *ARX 428_451dup24* mutation (Table 1) thus completing the initial description of 27 patients previously published (19). First, we observed that 47.6% of the *ARX* patients presented with hyperactivity and stereotyped behavior (scores above the 50th percentile threshold on the Nisonger's scale). Only 14.3% of *ARX* patients were assessed as being calm and 42.9% of them were also recorded with conduct disorder score (not following rules, temper tantrums, fights with other children) above the 50th percentile threshold on the Nisonger's scale. Stereotyped behavior manifested by rocking body or head back and forth repetitively, hitting or slapping patient's own head, neck, hands or other body parts, and repeatedly biting self, hard enough to leave tooth marks or break skin. Adaptive skills of *ARX* patients were assessed using the Vineland adaptive behavioral scale and showed a perfectly adequate interpersonal relationships in 56.3% of them despite their ID [mean global score on Vineland: 41, SD:15, (20–70)]. Only 71% of *ARX* patients had some level of anxiety (with a score above the 50th percentile), however, only 19% of them presented with severe anxiety (with a score above the 80th percentile on the Nisonger's scale). Only 11% of *ARX* patients had a depressive episode, a percentage lower than the general population lifetime prevalence (19–21% in France; 37).

Regarding their learning and memory abilities, their working memory was in accordance with their general cognitive abilities (their working memory index was not significantly different from their total IQ on Wechsler scales).

Neurological and motor examination of *ARX* patients did not show any spasticity, nor motor deficit. Fine motor skills were impaired in all patients with a range of severity; strikingly, patient's hand grasping was very specific. *ARX* patients scored higher on the balance subtest of the Lincoln-Oseretsky motor development scale (LOMDS) than IQ- and age-matched Down syndrome (DS) patients ($t = 3.5$, $P = 0.003$, Student *t*-test). Moreover, a writing speed test showed that they were significantly more impaired than DS patients (age- and IQ-matched) with 25 letters copied on average for *ARX* patients and 40 letters copied for DS patients ($t = 2.1$, $P < 0.05$, Student *t*-test).

Epilepsy manifestations were observed in 11 of the 33 *ARX c.428_451dup24* patients. Three out of the 33 *ARX c.428_451dup24* patients (9.1%) presented with West syndrome [i.e. infantile spasms, psychomotor regression and hypsarythmia on the electroencephalography (EEG)] with a mean age onset of 5 months, [4–7]. The other eight patients showed various types of seizures including absence, complex partial seizures and generalized tonic-clonic seizures with a mean age onset of 10.1 years, [1.8–33]. Only three patients required multiple antiepileptic treatment. It was possible after a few years to stop the antiepileptic treatment in five patients.

Discussion

We describe here the characterization of a new mouse model partially humanized for the *ARX c.428_451dup24* duplication, leading to polyalanine expansion in ARX tract 2. Our mouse

model supports previous findings showing that this mutation causes a decreased expression of *Arx* (23,27,38). It has been shown that polyalanine expansions cause inappropriate oligomerization of the protein, which is targeted for clearance by the cellular quality-control machinery (24,39), thus possibly explaining the decreased amount of ARX protein that we observed both in western blot (Fig. 1E) and by immunohistochemistry (Supplementary Material, Fig. S2). However, this does not explain ~12% decreased amount of mRNA that we observed both at E15.5 and adult stage. Interestingly, we found that the 24 bp duplication leads to DNA instability of the polyalanine tract 2 (see Supplementary Material, Fig. S1), with the recurrent apparition of products of smaller and larger size but always in frame, suggesting that they are not the result of a technical bias due to PCR amplification. Unfortunately, we were not able to detect the corresponding proteins by western blot, either due to a lack of sensitivity of the antibody (as the amount of these products is very low compared to the 24 bp duplication mutated protein) or because these mRNAs may be unstable and thus degraded. This last hypothesis would give a possible explanation for the decreased amount of *Arx* mRNA observed. Alternatively, it could also be a direct consequence of the presence of 24 bp duplication that would make the mRNA less stable. Interestingly, this instability was also found in *ARX c.428_451dup24* patient DNA extracted from blood cells, suggesting that the same situation also occurs in human.

The behavioral defects observed in the partially humanized $Arx^{dup24/0}$ mouse model are strikingly similar to the symptoms observed in *ARX c.428_451dup24* patients (Table 1), as far as human/mouse neurobehavioral phenotypes can be compared. *ARX* patients have initially been described with a strong phenotypic heterogeneity. However, a recent clinical re-evaluation of 27 patients from 12 different families, confirmed by the present description of 6 additional patients, all evaluated by the same clinician, revealed that this mutation constitutes a recognizable clinical syndrome with ID, an oro-lingual apraxia and a very specific upper limb distal motor apraxia with a very specific hand grasping but a normal gross motor function (19; this study). We observed good correspondence between $Arx^{dup24/0}$ mice and *ARX* patients concerning hyperactivity and stereotypy manifestations. Strikingly, the percentage of $Arx^{dup24/0}$ P7-P11 pups presenting infantile spasms (8%) was very similar to the 9.1% of *ARX* patients presenting with West syndrome (Table 1). However, we remarked differences concerning the manifestation of anxiety (most *ARX* patients had some level of anxiety whose only a minority had severe anxiety, whereas $Arx^{dup24/0}$ mice had similar level of anxiety than $Arx^{wt/0}$ mice, although the presence of hyperactivity and stereotypy in new environments may reveal some level of anxiety). No change was noted in working or spatial memory, but we observed alteration in contextual memory for fear in mice. The hyperactivity and the alteration in associative memory in $Arx^{dup24/0}$ mice are very similar to the phenotypes described for $Dlx1^{-/-}$ mutant mice (40,41), and thus consistent with a defect in interneuron development. Similarly to *ARX* patients, $Arx^{dup24/0}$ mutant mice have good performance in the gross motor coordination as revealed in the rotarod test, whereas they presented with fine motor defects in the MoRaG test, automated gait analysis and the beam walking test, more suggestive of an alteration of gait and proprioceptive and fine motor abilities. It is interesting to note that motor defects were more easily detected in mutant mice than defects in learning and memory abilities. This is possibly due to the better sensitivity of mouse tests assessing locomotor functions than neuropsychological tests which would allow only the detection of severe phenotypes in mice. Moreover, *ARX c.428_451dup24* patients are considered to have mild ID, thus, although we detected an associative memory phenotype in mice, the cognitive phenotypes could be too mild to be significantly detected using the current battery of tests.

Previously, two mouse models for the expansion in the polyalanine tract 1 [*c.304ins(GCG)*$_7$] have been described (22,23). These mouse models displayed infantile motor spasms, severe seizures, distinctive EEG abnormalities and cognitive and behavioral abnormalities, such as impaired associative learning, abnormal social interaction and contradictory results concerning anxiety (22,23). Interestingly, our mouse model presents similarities with these *Arx c.304ins(GCG)*$_7$ mouse models, in particular concerning the infantile spams and the alteration in associative learning. However, it shows several differences, suggestive of a milder phenotype, with a smaller proportion of animals presenting infantile spontaneous motor spasms [5 affected over 15 pups for the *Arx c.304ins(GCG)*$_7$ mouse model and only 2 affected over 25 pups for our *Arx c.428_451dup24* mouse model], the absence of increased susceptibility to induced epilepsy for *Arx c.428_451dup24* mouse model and the fear conditioning test for which *Arx c.304ins(GCG)*$_7$ mice present alteration in both the cue and the contextual memories (22,23) whereas *Arx c.428_451dup24* mouse model is only affected for contextual memory. Those results are in agreement with what has been reported for human patients presenting *ARX c.428_451dup24* mutations who are described as less severely affected than patients with *ARX c.304ins(GCG)7* expansion (28,42,43). Another mouse model for *ARX c.428_451dup24* mutation has been recently described with much more pronounced spontaneous seizures activity than our model (38). This difference may be due to a different environmental condition affecting the animals. This model was generated by Kitamura *et al.* (23) on 129SV ES cells and then bred on C57BL/6J (B6J) and backcrossed on C57BL/6NHsd (B6NHsd) genetic background in Jackson's publication (38). The only difference with our model is that the latter was backcrossed on B6NTac genetic background. Thus, we may propose that the B6NHsd are more prone to seizures than the B6NTac. Indeed, differences in epilepsy and death susceptibility after pro-convulsant injection have been reported between different B6N strains (44). However, it is interesting to note that originally, when Kitamura *et al.* (23) first published this mouse model, they did not observe any particular phenotype including epilepsy. In addition, the phenotype we observed in our mouse model is much closer to the rather mild phenotype observed in the patients, especially concerning the frequency and severity of infantile spasms and epilepsy. The most striking features of our mouse model is that it also recapitulates the fine motor defects which is a common hallmark of *ARX c.428_451dup24* patients (19).

Comparison of our RNA-seq results performed on E15.5 $Arx^{dup24/0}$ and $Arx^{wt/0}$ forebrains with published databases revealed a global decreased expression of genes important for interneuron development and/or migration (Fig. 3). Accordingly, we found defects in interneuron subpopulations, especially in the number and distribution of CB+, CR+ and ChAT+ cells at E15.5. At P0, we showed an accumulation of IN in the periphery of the CP and a decreased proportion in the center of the CP. This observation may be caused by IN being delayed to penetrate cortical layers by radial migration (as previously suggested for Arx knockout mice; (2)). A defect in neuronal migration is further strengthened by the enrichment of genes involved in cell migration among deregulated genes in E15.5 $Arx^{dup24/0}$ mice ($P = 4.11 \times 10^{-11}$, ingenuity pathway analysis). Eventually, the

IN distribution defects in our mouse model were partially compensated at adult stage, although the distribution of some interneuron subpopulations was still impaired in adult cortex. Interestingly, interneuron subpopulations affected in $Arx^{dup24/0}$ mutant mice were very similar to the ones affected in *Arx* mouse models for other mutations (2,9,13,22,23,45,46). Finally, it is interesting to draw a parallel between IN alterations in the striatum and the cortex (including the motor cortex) and the fine motor alterations. It has been shown that the cortical to basal ganglia (which include the striatum) interconnections play key function in motor learning and in coordinated voluntary motor movements (47). Strikingly, we found a decrease in the volume of some basal ganglia nuclei (in particular the caudate nucleus) in *ARX c.428_451dup24* patients, and we noted a correlation between the volume reduction and patients' motor impairment severity (Curie, Friocourt *et al*., submitted), reinforcing the importance of subpallial development in the peculiar fine motor defects observed in these patients.

Phospho-H3 labeling in the GE did not show any significant difference of the number of dividing progenitors in $Arx^{dup24/0}$ mice compared to $Arx^{wt/0}$ mice. However, when comparing our RNA-seq dataset with a recently published one on medial ganglionic eminence (MGE)-derived cellular populations at different embryonic stages (48), we observed a global increased expression of genes normally expressed in MGE proliferating neural progenitors (such as *Cenpf*, *Ccnb2*, *Ccnb1*, *Mcm5*, *Lhx5*, *Hes1*, *Notch1*, *Notch2*, *Nde1*, *Cdca3*, *Cdca8* and *Psat1*) and a tendency of decreased expression of genes normally expressed in MGE postmitotic immature neurons (such as *Nrxn3*, *Celf5*, *Gad1*, *Stmn2*, *Stmn3*, *Celf5*, *Dnm3* and *Cxx1c*) in $Arx^{dup24/0}$ E15.5 embryos, suggesting a global delay in the generation/maturation of MGE neurons that may be compensated at later stages. The MGE produces cortical INs, but also contributes to the generation of striatal interneurons and cholinergic neurons and pallial projection neurons (49,50). This defect may also concern the lateral ganglionic eminence (LGE) (responsible for the production of majority of striatal neurons) and caudal ganglionic eminence (CGE) (responsible for the production of neurons of cortex, amygdala and hippocampus) but it is difficult to tell just from RNA-seq results, as these three structures lack specific gene signature (51,52). Thereby, an alteration of the generation/maturation of the MGE, LGE and CGE neurons would explain the decreased number of different neuron types, namely CB+, CR+ and ChAT+ cells observed in the cortex and subpallial structures at E15.5, and the decreased expression of genes important for striatal neuron development such as *Foxp1*, *Drd1* and *Tac1* (Fig. 3D). Further analysis using different protein markers or *in situ* hybridization probes will be necessary to fully characterize this maturation delay. Finally, as impaired interneuron function was also suggested by epilepsy manifestations both in $Arx^{dup24/0}$ pups and *ARX c.428_451dup24* patients, we thus investigated the consequences of a defect in interneuron migration and/or development at adult stage by analyzing electrophysiological properties at hippocampal to BLA connections. We detected an alteration of I/E balance, which is interesting to correlate with the alteration observed in the contextual fear conditioning as efficient hippocampal projections to the BLA have been shown to be crucial for the aversive conditioned response in mice (36).

Arx was shown to be also important for excitatory neuron development (34,35,53,54), thus we also looked at markers of pyramidal neurons. The slight decreased in the number of Tbr1+ cells observed at E15.5 suggests that the global delay of neuronal generation/maturation suspected in GE may also be present in this neuronal population. However, we did not detect any change in the expression or localization of Pax6 or Tbr2+ cells in the cortex. Further studies would be required to fully investigate this aspect. However, the absence of increased susceptibility to induced epilepsy in $Arx^{dup24/0}$ adult males is not in favor of major defects in pyramidal neurons.

In conclusion, our new mouse model expressing the human *ARX c.428_451dup24* mutation appears as a relevant model to further dissect the pathophysiological effects of this mutation and for the development of therapeutic approaches, as it shows striking similarities with human patients, especially in behavior with hyperactivity and defects in fine motor and proprioceptive abilities. It highlights alteration of generation, migration and functioning of interneurons in various regions of the brain as a direct consequence of 24 bp duplication effect on *Arx* function. Even if most of adult interneurons recover their position, the rescue is not complete, inducing a series of changes in the overall activity, a defect in associative learning and in controlling fine motor movements.

Materials and Methods

Mouse line and ethical statement

The $Arx^{KI.ICS}$ mutant mouse line (noted $Arx^{dup24/0}$) was generated and analyzed in the mouse genetic background C57BL/6N*129Sv/Pas*C57BL/6J (95.3*3.1*1.5%, Supplementary Material, Fig. 1A and B). All mouse experimental procedures were performed in agreement with the EC directive 2010/63/UE86/609/CEE for the care and use of laboratory animals and every effort was made to minimize the number of animals used and their suffering. The behavioral pipeline was approved by the local animal care, use and ethic committee of the Institute of Genetics and of Molecular and Cellular Biology (IGBMC) under accreditation number 2012-139. The experimental design and procedures of electrophysiological experiments were performed in accordance with the animal care guidelines issued by the animal experimental committee of Bordeaux Universities (CE50, A5012009).

Behavioral experiments

Five cohorts of $Arx^{wt/0}$ and $Arx^{dup24/0}$ male mice were used for behavioral experiments (8–15 per genotype and per cohort) and 9–31 weeks old mice were tested for circadian activity, general health, basic neurological reflexes, anxiety related behavior, susceptibility to despair, learning and memory (emotional, spatial), working memory, social recognition, proprioceptive abilities, specific motor abilities, gait analysis and susceptibility to epileptic seizures. One cohort of P7–P11 pups (25 mutants and 34 controls males) were investigated for spontaneous infantile spasms. The behavioral tests and cohorts used are described in the Supplementary Material.

Electrophysiology

All electrophysiological experiments were performed on 2 months old males (five $Arx^{dup24/0}$ and three $Arx^{wt/0}$ littermates). Mice were injected in the caudal hippocampus with adeno-associated viruses (AAV) containing the channel rhodopsin gene ChR2. After waiting 4 weeks for ChR2 gene expression, we prepared coronal BLA-containing acute slices from infected mice and recorded neurons visualized with infrared video microscopy in the voltage clamp mode at −70 mV [to record AMPAR-mediated excitatory postsynaptic currents (EPSCs)]

or 0 mV (to record $GABA_AR$-mediated inhibitory postsynaptic currents) (36). Hippocampo-BLA monosynaptic EPSCs and disynaptic inhibitory postsynaptic currents were elicited by 1 ms light-stimulations. Details of the electrophysiological procedures used are described in the Supplementary Material.

RNA-seq libraries and analysis

Total RNA was Trizol-extracted from three wild-type and three mutant frozen embryonic forebrains (including developing cortex and basal ganglia). All steps of RNA treatment and cDNA preparation are described in the Supplementary Material. The RNA-seq libraries were synthetized with KAPA Hyper prep kit and sequenced on Illumina HiSeq and mapped with GSNAP (version 2015–06-23), which yielded on average 51.1 mapped million (single-end) reads per sample. Gene expression counts (tags only in exons, not introns) were given as input to DEseq2 to call the dysregulated genes. Data were deposited in GEO (ID GSE90036). RNA-seq results were compared with the published datasets (31–33) by means of hypergeometric test with Bonferroni correction. Specifically, (i) we estimated the background genes by selecting the common annotations between the RNA-seq dataset (RefSeq annotations) and each microarray of the published datasets; (ii) we obtained the lists of deregulated genes in the published datasets by selecting the genes with fold-change superior to two according to the values available in the Supplementary Materials and (iii) we computed hypergeometric test with Bonferroni correction.

Immunohistochemistry on brain sections and cell counting

Brains from 13-week-old, post-natal day 0 (P0) and day-post-coïtum 15.5 (E15.5) $Arx^{dup24/0}$ and $Arx^{wt/0}$ males (4–6 of each genotype) were harvested as described elsewhere (55). Antibodies and immunohistochemistry procedures are described in the Supplementary Material.

ARX c.*428_451dup24* patients

After explaining the aims of the study, all patients and their guardians gave written informed consent for the study, which was approved by the Ethical Committee of French Public Hospitals (Comité de Protection des Personnes Lyon-Sud Est II, 2010-A00327–32, 09/22/2010).

Supplementary Material

Supplementary Material is available at *HMG* online.

Acknowledgements

We would like to thank ARX *c.428_451dup24* patients who participated to this study and Vincent des Portes and Renaud Touraine for patients' recruitment, clinical examination and DNA samples; the Genetic Engineering and Model Validation Department for generating the mouse model; Alain Guimond and Christophe Mittelhaeuser from the behavioral platform and the animal care-takers of the PHENOMIN-ICS animal facility for their technical assistance with mouse care.

Conflict of Interest statement. None declared.

Funding

EU funded project 'Genetic and Epigenetic Networks in Cognitive Dysfunction' (GENCODYS) consortium (http://www.gencodys.eu/) (FP7-COLLABORATION PROJECT-2009–2.1.1-1/241995 to H.S and Y.H.); French state funds through the 'Agence Nationale de la Recherche' under the frame programme Investissements d'Avenir labeled (ANR-10-IDEX-0002–02, ANR-10-LABX-0030-INRT, ANR-10-INBS-07 PHENOMIN to Y.H.); Jérôme Lejeune Foundation (2007–2014 to G.F.), IBSAM (2016–2017 to G.F.); Gaétan Saleün Association (to G.F.). The funders had no role in the study design, data collection and analysis, decision to publish or manuscript preparation. Funding to pay the Open Access publication charges for this article was provided by Y.H.

References

1. Dobyns, W.B., Truwit, C.L., Ross, M.E., Matsumoto, N., Pilz, D.T., Ledbetter, D.H., Gleeson, J.G., Walsh, C.A. and Barkovich, A.J. (1999) Differences in the gyral pattern distinguish chromosome 17-linked and X-linked lissencephaly. *Neurology*, **53**, 270–277.
2. Kitamura, K., Yanazawa, M., Sugiyama, N., Miura, H., Iizuka-Kogo, A., Kusaka, M., Omichi, K., Suzuki, R., Kato-Fukui, Y. and Kamiirisa, K. (2002) Mutation of ARX causes abnormal development of forebrain and testes in mice and X-linked lissencephaly with abnormal genitalia in humans. *Nat. Genet.*, **32**, 359–369.
3. Bonneau, D., Toutain, A., Laquerriere, A., Marret, S., Saugier-Veber, P., Barthez, M.A., Radi, S., Biran-Mucignat, V., Rodriguez, D. and Gelot, A. (2002) X-linked lissencephaly with absent corpus callosum and ambiguous genitalia (XLAG): clinical, magnetic resonance imaging, and neuropathological findings. *Ann. Neurol.*, **51**, 340–349.
4. Kato, M., Das, S., Petras, K., Kitamura, K., Morohashi, K., Abuelo, D.N., Barr, M., Bonneau, D., Brady, A.F., Carpenter, N.J. *et al.* (2004) Mutations of ARX are associated with striking pleiotropy and consistent genotype-phenotype correlation. *Hum. Mutat.*, **23**, 147–159.
5. Friocourt, G., Poirier, K., Rakic, S., Parnavelas, J.G. and Chelly, J. (2006) The role of ARX in cortical development. *Eur. J. Neurosci.*, **23**, 869–876.
6. Friocourt, G. and Parnavelas, J.G. (2010) Mutations in ARX result in several defects involving GABAergic neurons. *Front. Cell Neurosci.*, **4**, 4.
7. Shoubridge, C., Fullston, T. and Gecz, J. (2010) ARX spectrum disorders: making inroads into the molecular pathology. *Hum. Mutat.*, **31**, 889–900.
8. Poirier, K., Van Esch, H., Friocourt, G., Saillour, Y., Bahi, N., Backer, S., Souil, E., Castelnau-Ptakhine, L., Beldjord, C., Francis, F. *et al.* (2004) Neuroanatomical distribution of ARX in brain and its localisation in GABAergic neurons. *Brain Res. Mol. Brain Res.*, **122**, 35–46.
9. Colombo, E., Collombat, P., Colasante, G., Bianchi, M., Long, J., Mansouri, A., Rubenstein, J.L. and Broccoli, V. (2007) Inactivation of Arx, the murine ortholog of the X-linked lissencephaly with ambiguous genitalia gene, leads to severe disorganization of the ventral telencephalon with impaired neuronal migration and differentiation. *J. Neurosci.*, **27**, 4786–4798.
10. Colasante, G., Collombat, P., Raimondi, V., Bonanomi, D., Ferrai, C., Maira, M., Yoshikawa, K., Mansouri, A., Valtorta, F., Rubenstein, J.L. *et al.* (2008) Arx is a direct target of Dlx2 and thereby contributes to the tangential migration of GABAergic interneurons. *J. Neurosci.*, **28**, 10674–10686.

11. Cobos, I., Broccoli, V. and Rubenstein, J.L. (2005) The vertebrate ortholog of aristaless is regulated by Dlx genes in the developing forebrain. *J. Comp. Neurol.*, **483**, 292–303.
12. Stuhmer, T., Anderson, S.A., Ekker, M. and Rubenstein, J.L. (2002) Ectopic expression of the Dlx genes induces glutamic acid decarboxylase and Dlx expression. *Development*, **129**, 245–252.
13. Fulp, C.T., Cho, G., Marsh, E.D., Nasrallah, I.M., Labosky, P.A. and Golden, J.A. (2008) Identification of Arx transcriptional targets in the developing basal forebrain. *Hum. Mol. Genet.*, **17**, 3740–3760.
14. Quille, M.L., Carat, S., Quemener-Redon, S., Hirchaud, E., Baron, D., Benech, C., Guihot, J., Placet, M., Mignen, O., Ferec, C. *et al.* (2011) High-throughput analysis of promoter occupancy reveals new targets for Arx, a gene mutated in mental retardation and interneuronopathies. *PLoS One*, **6**, e25181.
15. Colasante, G., Sessa, A., Crispi, S., Calogero, R., Mansouri, A., Collombat, P. and Broccoli, V. (2009) Arx acts as a regional key selector gene in the ventral telencephalon mainly through its transcriptional repression activity. *Dev. Biol.*, **334**, 59–71.
16. Friocourt, G. and Parnavelas, J.G. (2011) Identification of Arx targets unveils new candidates for controlling cortical interneuron migration and differentiation. *Front. Cell Neurosci.*, **5**, 28.
17. McKenzie, O., Ponte, I., Mangelsdorf, M., Finnis, M., Colasante, G., Shoubridge, C., Stifani, S., Gecz, J. and Broccoli, V. (2007) Aristaless-related homeobox gene, the gene responsible for West syndrome and related disorders, is a Groucho/transducin-like enhancer of split dependent transcriptional repressor. *Neuroscience*, **146**, 236–247.
18. Gecz, J., Cloosterman, D. and Partington, M. (2006) ARX: a gene for all seasons. *Curr. Opin. Genet. Dev.*, **16**, 308–316.
19. Curie, A., Nazir, T., Brun, A., Paulignan, Y., Reboul, A., Delange, K., Cheylus, A., Bertrand, S., Rochefort, F., Bussy, G. *et al.* (2014) The c.429_452 duplication of the ARX gene: a unique developmental-model of limb kinetic apraxia. *Orphanet. J. Rare Dis.*, **9**, 25.
20. Nasrallah, I.M., Minarcik, J.C. and Golden, J.A. (2004) A polyalanine tract expansion in Arx forms intranuclear inclusions and results in increased cell death. *J. Cell Biol.*, **167**, 411–416.
21. Shoubridge, C., Cloosterman, D., Parkinson-Lawerence, E., Brooks, D. and Gecz, J. (2007) Molecular pathology of expanded polyalanine tract mutations in the aristaless-related homeobox gene. *Genomics*, **90**, 59–71.
22. Price, M.G., Yoo, J.W., Burgess, D.L., Deng, F., Hrachovy, R.A., Frost, J.D., Jr and Noebels, J.L. (2009) A triplet repeat expansion genetic mouse model of infantile spasms syndrome, Arx(GCG)10+7, with interneuronopathy, spasms in infancy, persistent seizures, and adult cognitive and behavioral impairment. *J. Neurosci.*, **29**, 8752–8763.
23. Kitamura, K., Itou, Y., Yanazawa, M., Ohsawa, M., Suzuki-Migishima, R., Umeki, Y., Hohjoh, H., Yanagawa, Y., Shinba, T., Itoh, M. *et al.* (2009) Three human ARX mutations cause the lissencephaly-like and mental retardation with epilepsy-like pleiotropic phenotypes in mice. *Hum. Mol. Genet.*, **18**, 3708–3724.
24. Polling, S., Ormsby, A.R., Wood, R.J., Lee, K., Shoubridge, C., Hughes, J.N., Thomas, P.Q., Griffin, M.D., Hill, A.F., Bowden, Q. *et al.* (2015) Polyalanine expansions drive a shift into alpha-helical clusters without amyloid-fibril formation. *Nat. Struct. Mol. Biol.*, **22**, 1008–1015.
25. Seufert, D.W., Prescott, N.L. and El-Hodiri, H.M. (2005) Xenopus aristaless-related homeobox (xARX) gene product functions as both a transcriptional activator and repressor in forebrain development. *Dev. Dyn.*, **232**, 313–324.
26. Nasrallah, M.P., Cho, G., Simonet, J.C., Putt, M.E., Kitamura, K. and Golden, J.A. (2012) Differential effects of a polyalanine tract expansion in Arx on neural development and gene expression. *Hum. Mol. Genet.*, **21**, 1090–1098.
27. Lee, K., Mattiske, T., Kitamura, K., Gecz, J. and Shoubridge, C. (2014) Reduced polyalanine-expanded Arx mutant protein in developing mouse subpallium alters Lmo1 transcriptional regulation. *Hum. Mol. Genet.*, **23**, 1084–1094.
28. Stromme, P., Mangelsdorf, M.E., Shaw, M.A., Lower, K.M., Lewis, S.M., Bruyere, H., Lutcherath, V., Gedeon, A.K., Wallace, R.H., Scheffer, I.E. *et al.* (2002) Mutations in the human ortholog of aristaless cause X-linked mental retardation and epilepsy. *Nat. Genet.*, **30**, 441–445.
29. Collins, R.L. (1968) On the inheritance of handedness. I. Laterality in inbred mice. *J. Hered.*, **59**, 9–12.
30. Collins, R.L. (1969) On the inheritance of handedness. II. *Selection for Sinistrality in Mice. J. Hered.*, **60**, 117–119.
31. Marsh, E.D., Minarcik, J., Campbell, K., Brooks-Kayal, A.R. and Golden, J.A. (2008) FACS-array gene expression analysis during early development of mouse telencephalic interneurons. *Dev. Neurobiol.*, **68**, 434–445.
32. Batista-Brito, R., Machold, R., Klein, C. and Fishell, G. (2008) Gene expression in cortical interneuron precursors is prescient of their mature function. *Cereb. Cortex*, **18**, 2306–2317.
33. Zeisel, A., Munoz-Manchado, A.B., Codeluppi, S., Lonnerberg, P., La Manno, G., Jureus, A., Marques, S., Munguba, H., He, L., Betsholtz, C. *et al.* (2015) Cell types in the mouse cortex and hippocampus revealed by single-cell RNA-seq. *Science*, **347**, 1138–1142.
34. Friocourt, G., Kanatani, S., Tabata, H., Yozu, M., Takahashi, T., Antypa, M., Raguenes, O., Chelly, J., Ferec, C., Nakajima, K. *et al.* (2008) Cell-autonomous roles of ARX in cell proliferation and neuronal migration during corticogenesis. *J. Neurosci.*, **28**, 5794–5805.
35. Colasante, G., Simonet, J.C., Calogero, R., Crispi, S., Sessa, A., Cho, G., Golden, J.A. and Broccoli, V. (2015) ARX regulates cortical intermediate progenitor cell expansion and upper layer neuron formation through repression of Cdkn1c. *Cereb. Cortex*, **25**, 322–335.
36. Zhang, C.L., Houbaert, X., Lepleux, M., Deshors, M., Normand, E., Gambino, F., Herzog, E. and Humeau, Y. (2015) The hippocampo-amygdala control of contextual fear expression is affected in a model of intellectual disability. *Brain Struct. Funct.*, **220**, 3673–3682.
37. Kessler, R.C. and Bromet, E.J. (2013) The epidemiology of depression across cultures. *Annu. Rev. Public Health*, **34**, 119–138.
38. Jackson, M.R., Lee, K., Mattiske, T., Jaehne, E.J., Ozturk, E., Baune, B.T., O'Brien, T.J., Jones, N. and Shoubridge, C. (2017) Extensive phenotyping of two ARX polyalanine expansion mutation mouse models that span clinical spectrum of intellectual disability and epilepsy. *Neurobiol. Dis.*, **105**, 245–256.
39. Messaed, C. and Rouleau, G.A. (2009) Molecular mechanisms underlying polyalanine diseases. *Neurobiol. Dis.*, **34**, 397–405.
40. Mao, R., Page, D.T., Merzlyak, I., Kim, C., Tecott, L.H., Janak, P.H., Rubenstein, J.L. and Sur, M. (2009) Reduced conditioned fear response in mice that lack Dlx1 and show subtype-specific loss of interneurons. *J. Neurodev. Disord.*, **1**, 224–236.
41. Cobos, I., Calcagnotto, M.E., Vilaythong, A.J., Thwin, M.T., Noebels, J.L., Baraban, S.C. and Rubenstein, J.L. (2005) Mice

lacking Dlx1 show subtype-specific loss of interneurons, reduced inhibition and epilepsy. *Nat. Neurosci.*, **8**, 1059–1068.
42. Stromme, P., Mangelsdorf, M.E., Scheffer, I.E. and Gecz, J. (2002) Infantile spasms, dystonia, and other X-linked phenotypes caused by mutations in aristaless related homeobox gene, ARX. *Brain Dev.*, **24**, 266–268.
43. Marques, I., Sá, M.J., Soares, G., Mota Mdo, C., Pinheiro, C., Aguiar, L., Amado, M., Soares, C., Calado, A., Dias, P. *et al.* (2015) Unraveling the pathogenesis of ARX polyalanine tract variants using a clinical and molecular interfacing approach. *Mol. Genet. Genomic. Med.*, **3**, 203–214.
44. Muller, C.J., Groticke, I., Hoffmann, K., Schughart, K. and Loscher, W. (2009) Differences in sensitivity to the convulsant pilocarpine in substrains and sublines of C57BL/6 mice. *Genes. Brain Behav.*, **8**, 481–492.
45. Marsh, E., Fulp, C., Gomez, E., Nasrallah, I., Minarcik, J., Sudi, J., Christian, S.L., Mancini, G., Labosky, P., Dobyns, W. *et al.* (2009) Targeted loss of Arx results in a developmental epilepsy mouse model and recapitulates the human phenotype in heterozygous females. *Brain*, **132**, 1563–1576.
46. Marsh, E.D., Nasrallah, M.P., Walsh, C., Murray, K.A., Nicole Sunnen, C., McCoy, A. and Golden, J.A. (2016) Developmental interneuron subtype deficits after targeted loss of Arx. *BMC Neurosci.*, **17**, 35.
47. Prodoehl, J., Corcos, D.M. and Vaillancourt, D.E. (2009) Basal ganglia mechanisms underlying precision grip force control. *Neurosci. Biobehav. Rev.*, **33**, 900–908.
48. Chen, Y.J., Friedman, B.A., Ha, C., Durinck, S., Liu, J., Rubenstein, J.L., Seshagiri, S. and Modrusan, Z. (2017) Single-cell RNA sequencing identifies distinct mouse medial ganglionic eminence cell types. *Sci. Rep.*, **7**, 45656.
49. Flandin, P., Kimura, S. and Rubenstein, J.L. (2010) The progenitor zone of the ventral medial ganglionic eminence requires Nkx2-1 to generate most of the globus pallidus but few neocortical interneurons. *J. Neurosci.*, **30**, 2812–2823.
50. Marín, O., Anderson, S.A., and Rubenstein, J.L.R. (2000) Origin and molecular specification of striatal interneurons. *J. Neurosci.*, **20**, 6063–6076.
51. Willi-Monnerat, S., Migliavacca, E., Surdez, D., Delorenzi, M., Luthi-Carter, R. and Terskikh, A.V. (2008) Comprehensive spatiotemporal transcriptomic analyses of the ganglionic eminences demonstrate the uniqueness of its caudal subdivision. *Mol. Cell Neurosci.*, **37**, 845–856.
52. Tucker, E.S., Segall, S., Gopalakrishna, D., Wu, Y., Vernon, M., Polleux, F. and Lamantia, A.S. (2008) Molecular specification and patterning of progenitor cells in the lateral and medial ganglionic eminences. *J. Neurosci.*, **28**, 9504–9518.
53. Beguin, S., Crépel, V., Aniksztejn, L., Becq, H., Pelosi, B., Pallesi-Pocachard, E., Bouamrane, L., Pasqualetti, M., Kitamura, K., Cardoso, C. and Represa, A. (2013) An epilepsy-related ARX polyalanine expansion modifies glutamatergic neurons excitability and morphology without affecting GABAergic neurons development. *Cereb. Cortex*, **23**, 1484–1494.
54. Simonet, J.C., Sunnen, C.N., Wu, J., Golden, J.A. and Marsh, E.D. (2015) Conditional loss of Arx from the developing dorsal telencephalon results in behavioral phenotypes resembling mild human ARX mutations. *Cereb. Cortex*, **25**, 2939–2950.
55. Dubos, A., Castells-Nobau, A., Meziane, H., Oortveld, M.A.W., Houbaert, X., Iacono, G., Martin, C., Mittelhaeuser, C., Lalanne, V., Kramer, J.M. *et al.* (2015) Conditional depletion of intellectual disability and Parkinsonism candidate gene ATP6AP2 in fly and mouse induces cognitive impairment and neurodegeneration. *Hum. Mol. Genet.*, **24**, 6736–6755.